Development of Bioengineering Strategies for Periodontal Tissue Regeneration

Laura Sofia Alves[1]

Periodontitis is an inflammatory disease caused by dental plaque accumulation that can damage the periodontium, the complex structure that surrounds and supports the teeth. The periodontium is composed by hard (cementum and alveolar bone) and soft (periodontal ligament) tissues. In this work, a novel strategy for periodontal tissue regeneration, namely alveolar bone, was explored by combining human periodontal ligament stem cells (PDLSCs) with 3-dimensional (3D) printed polycaprolactone (PCL) scaffolds with different pore sizes (100 µm, 300 µm and 600 µm). Thus, we isolated and characterized PDLSCs from human teeth of healthy donors and compared the osteogenic potential of these cells with mesenchymal stromal cells (MSCs) derived from bone marrow (BMMSCs) and adipose tissue (ATMSCs). After isolation, PDLSCs were characterized regarding MSC marker expression, multilineage differentiation potential, morphology, and growth kinetics. Results demonstrated that PDLSCs presented MSC-like morphology, MSC-related marker expression (analyzed by flow cytometry), and multilineage differentiation capacity (adipogenic, chondrogenic and osteogenic). Despite this, immunocytochemistry assays showed that PDLSCs exhibited expression of osteopontin, osteocalcin, asporin, and Stro-1, while BMMSCs and ATMSCs did not. Moreover, PDLSCs expressed CD146 and presented higher proliferative potential than BMMSCs and ATMSCs. Furthermore, osteogenic potential of BMMSCs, ATMSCs and PDLSCs was evaluated. Results demonstrated that, after osteogenic differentiation, PDLSCs exhibited an enhanced upregulation of osteogenic/periodontal genes compared to ATMSCs and BMMSCs, such as *Runx2*, *Col I* and *CEMP-1*. However, ALP activity of PDLSCs did not increase after osteogenic differentiation. Lastly, PDLSCs were successfully cultured in 3D-printed PCL scaffolds with different pore sizes (100 µm, 300 µm and 600 µm). Results suggested that lower pore sizes (100 µm and 300 µm) favored PDLSC proliferation. Overall, the results showed that PDLSCs are a promising cell source for periodontal regeneration, presenting enhanced osteogenic potential and that PDLSCs can successfully proliferate in a 3D PCL scaffold with different pore sizes. Future studies should be performed to evaluate the osteogenic potential of PDLSCs in PCL scaffolds for alveolar bone regeneration applications.

Keywords: Alveolar Bone, Mesenchymal Stromal Cells, Periodontal Ligament Stem Cells, Periodontium, Polycaprolactone

1. Introduction

The periodontium is a dynamic structure composed by specialized tissues that surround the tooth and provide attachment to the bone of the jaw [1]. Periodontium is composed by several tissues: alveolar bone, cementum and periodontal ligament (PDL). Cementum is a hard, avascular connective tissue that surrounds the tooth root, attaching it to the PDL fibers [1]. The alveolar bone is a mineralized tissue that arises from the maxilla or mandible and is the part of the bone that contains the sockets for the teeth [1]. The PDL is a highly cellular fibrous connective tissue, located between the alveolar bone and the cementum covering the root. By connecting the tooth root to the bone surface, PDL collagen fibers are critical for tooth support and attachment [1]. Thus, periodontal homeostasis and regeneration require the formation of new cementum, alveolar bone and PDL [2,3].

Periodontitis is an inflammatory disease that can damage the periodontium triggered by pathogenic microorganisms that arise from dental plaque accumulation. Severe periodontitis can result in occasional pain and discomfort, impaired mastication, and eventual tooth loss [4,5]. The key destructive events of periodontitis are caused by the host-derived mediators and enzymes released by inflammatory cells in response to the microbial challenge posed by dental plaque accumulation. To accommodate the inflammatory and immune cells, destruction of structural components of the periodontium occurs by the action of matrix metalloproteinases that degrade the PDL collagen fibers. Additionally, the recruitment of macrophages that secrete prostaglandins, interleukins and tumor necrosis factor-α, results in osteoclast stimulation and consequential alveolar bone resorption. Ultimately, this leads to the formation of periodontal tissues pockets with damage in both hard and soft periodontal tissues, tooth attachment loss and bone loss [6].

Evidence suggested that the PDL include a population of undifferentiated stem cells that potentially act as a source of renewable progenitor cells, producing cementoblasts (cementum progenitors), osteoblasts (alveolar bone progenitors) and fibroblasts throughout adult life [7,8] . In 2004, Seo and colleagues successfully isolated cells with stem cell characteristics from the human PDL, PDL stem cells (PDLSCs), expressing a mesenchymal stromal cell (MSC) phenotype, including multilineage differentiation potential [9].

Regarding periodontal tissue regeneration, novel strategies have combined the delivery of PDLSCs to periodontal defects through biocompatible and biodegradable three-dimensional (3D) printed scaffolds. Thus, it can be possible to combine PDLSCs' regenerative potential with the structural support provided by 3D scaffolds designed according to alveolar bone defect anatomy. Aiming to investigate the potential of PDLSC application in alveolar bone tissue regeneration, the aim of the thesis project was: (i) to successful isolate and characterize PDLSCs; (ii) to compare the regenerative potential of PDLSCs with MSCs from other adult sources, such as bone marrow (BMMSCs) and adipose tissue (ATMSCs); (iii) to compare the osteogenic potential of PDLSCs with BMMSCs and ATMSCs; and lastly (iv) to successful culture PDLSCs on 3D printed PCL scaffolds and to optimize the pore size of PCL scaffolds to enhance PDLSC proliferation.

[1] The work herein presented is part of an MSc thesis project performed at the Institute for Bioengineering and Biosciences of Instituto Superior Técnico (Lisbon, Portugal), during the period March-November 2021, under the supervision of Dr. Marta Monteiro Silva Carvalho.

2. Materials and Methods

2.1. PDLSC Isolation and Culture

Healthy human third molars were extracted for orthodontic reasons from two healthy donors (20 and 28 years old). PDLSCs were isolated from the PDL according to the protocol proposed by Mrozik *et al.* in 2017. Samples were washed with wash buffer and the PDL was manually harvested with the aid of a surgical blade, washed, transferred into a 15 mL conical bottom tube, and centrifuged at 1500 rpm for 10 min at 18 °C. After discarding the supernatant, cells were digested in a solution of 3 mg/mL collagenase type I (Sigma-Aldrich) and 4 mg/mL dispase (Sigma-Aldrich) for 1 h at 37 °C. After neutralization with wash buffer, the digested tissue was strained through a 70 µm cell strainer to separate the undigested tissue from PDLSCs. PDL cells were finally separated by centrifugation at 1500 rpm for 10 min at 18 °C, resuspended in 2 mL of 10% FBS-containing DMEM growth media and plated in 6 well-plates. Adherent PDLSCs colonies were then harvested after reaching confluency and expanded in T-75 flasks using low-glucose Dulbecco's modified Eagle's medium (DMEM, Gibco) supplemented with 10% fetal bovine serum (FBS MSC qualified, Gibco) and 1% antibiotic-antimycotic (A/A, Gibco). Cells were kept at 37ºC, 5% CO_2 in a humidified atmosphere and medium renewal was performed every 3 days. Isolated cells were kept frozen in liquid/vapor nitrogen tanks until further use.

2.2. ATMSC and BMMSCS Cell Culture

ATMSCs and BMMSCs used in this work are part of the cell bank available at the Stem Cell Engineering Research Group (SCERG), Institute for Bioengineering and Biosciences (iBB) at Instituto Superior Técnico (IST). These MSCs were previously isolated/expanded according to protocols previously established at iBB-IST [11,12]. Human MSCs from different sources were thawed and plated on T-75 flasks using low-glucose DMEM supplemented with 10% FBS and 1% A/A and kept at 37 °C and 5% CO_2 in a humidified atmosphere. Medium renewal was performed every 3-4 days.

2.3. Multilineage Differentiation and Stainings

Osteogenic Differentiation: For osteogenic differentiation, ATMSCs, BMMSCs and PDLSCs were cultured at 3 x10^3 cells/cm^2 on 24-well plates with DMEM + 10% FBS. At 80% confluence, cells were incubated with osteogenic medium composed by low glucose DMEM supplemented with 10% FBS and 1% A/A, 10 mM β-glycerophosphate (Sigma-Aldrich), 10 nM dexamethasone (Sigma-Aldrich), and 50 µg/ml ascorbic acid (Sigma-Aldrich). Medium renewal was performed every 3-4 days. After 21 days of osteogenic differentiation, cultures were stained with alkaline phosphatase (ALP), von Kossa (VK), and Alizarin Red (AR) stainings.

ALP and VK stainings identify ALP activity (a known by-product of osteoblast activity) and mineralization, respectively, indicating the presence of active osteoblasts. Medium was removed and cells were washed with PBS. Cells were then fixed with 4% paraformaldehyde (PFA) (Sigma-Aldrich) solution for 15 min. Then, for the ALP staining, cells were rinsed with milliQ water and incubated with a Fast Violet solution (Sigma-Aldrich) and Naphthol AS-MX Phosphate alkaline solution (Sigma-Aldrich) in a final concentration of 4% for 45 min, at room temperature in the dark. Lastly, cells were washed and incubated with a 2.5% silver nitrate solution (Sigma-Aldrich) for 30 min at room temperature in the dark (von Kossa staining), followed by cell washing and imaging.

Alizarin Red staining was also performed to visualize calcium deposits. Cells were stained with a 2% AR solution (Sigma-Aldrich) by incubation for 1 h at room temperature. Afterwards, cells were washed with PBS and imaged.

Adipogenic Differentiation: ATMSCs, BMMSCs and PDLSCs were cultured at 3 x10^3 cells/cm^2 on 24-well plates with DMEM + 10% FBS. After reaching 80% confluency, adipogenic differentiation medium (StemPro™ Adipogenesis Differentiation Kit, Gibco) was added to the culture to induce differentiation into adipocytes. Medium was changed every 3-4 days and after 21 days of adipogenic differentiation, cells were fixed with 4% PFA for 15 min and stained with Oil Red O solution (0.3% in isopropanol) (Sigma-Aldrich) for 1 h at room temperature. Oil Red O stains accumulated lipids, allowing the detection of intracellular lipid droplet accumulation resulting from adipogenic differentiation. After staining, cells were washed with PBS and imaged.

Chondrogenic Differentiation: For chondrogenic differentiation, ATMSCs, BMMSCs and PDLSCs were cultured as cell aggregates. Cells were plated as small droplets (10 µl) at a cell density of 1x10^7 cells/ml on ultra-low attachment multi-well plates (Corning). Plates were placed in the incubator for 30 min and chondrogenic differentiation media (MesenCult™ Chondrogenic Differentiation Kit, Stemcell Technologies) was added. Medium was changed every 3-4 days and after 21 days of chondrogenic differentiation cells were fixed in 4% PFA for 15 min. These aggregates were stained with 1% Alcian Blue solution (Sigma-Aldrich) for 1 h, at room temperature. Alcian Blue stains glycosaminoglycans (GAGs), a known by-product of chondrocyte activity. Finally, aggregates were washed with PBS and imaged.

2.4. Flow Cytometry Analysis

Immunophenotypic analysis of BMMSCs, ATMSCs and PDLSCs was performed by flow cytometry using a panel of mouse anti-human monoclonal antibodies for the expression of CD14, CD19, CD29, CD34, CD44, CD45, CD73, CD80, CD90, CD105, CD106, CD146, CD166, HLA-DR and STRO-1 (BioLegend).

PDLSCs were analyzed from passages 1 to 7. ATMSCs and BMMSCs were analyzed in passages 3, 5, and 7. Briefly, cells (1x10^6 cells/ml) were incubated with each antibody for 20 min in the dark at room temperature. Afterwards, cells were washed with PBS and centrifuged at 1500 rpm for 5 min. Finally, cells were fixed using a solution of 4% PFA. A minimum of 10 000 events were collected for each sample. Flow cytometric analysis was performed using FACScalibur flow cytometer (Becton Dickinson) and CellQuest™ software (Becton Dickinson) was used for acquisition. For data analysis, Flowing Software (University of Turku, Finland) was used.

2.5. Immunocytochemistry Analysis

The presence and distribution of several ECM proteins, such as collagen I (Col I), asporin, fibronectin, laminin, osteopontin,

osteocalcin, cementum protein 1 and Stro-1, were analyzed in BMMSCs, ATMSCs and PDLSCs cultured under expansion (DMEM growth medium) and osteogenic differentiation conditions (osteogenic differentiation medium).

Cells were plated on 24-well plates and were fixed at two different timepoints: after reaching confluency (DMEM + 10% FBS) and after 21 days of osteogenic differentiation. Briefly, cells were washed with PBS and fixed with 4% PFA for 20 min at room temperature. Then, cells were washed with 1% bovine serum albumin (BSA, Sigma-Aldrich) in PBS and incubated for 45 min with a solution composed by 1% BSA, 10% FBS and 0.3% Triton X-100 in PBS to block and permeabilize cells. Primary antibodies (dilution 1:500 in 1% BSA, 10% FBS and 0.3% Triton X-100) including rabbit anti-human collagen I (Thermo Fisher Scientific), asporin (Abcam), laminin (Thermo Fisher Scientific), osteopontin (Abcam), osteocalcin (Sigma-Aldrich) and cementum protein 1 (Abcam) and mouse anti-human collagen IV (Thermo Fisher Scientific), fibronectin (Thermo Fisher Scientific) and stro-1 (Thermo Fisher Scientific) were added followed by overnight incubation at 4ºC. After washing with 1% BSA in PBS, goat anti-mouse IgG Alexa Fluor 546, goat anti-rabbit IgG Alexa Fluor 546 and goat anti-mouse IgG Alexa Fluor 488 (Thermo Fisher Scientific, dilution 1:200 in 1% BSA PBS solution) were used as secondary antibodies and incubated in the dark for 1 h at room temperature. Finally, the cell nuclei were counterstained with DAPI (Thermo Fisher Scientific, 1.5 µg/ml) for 5 min and then washed with PBS. Immunofluorescence staining was confirmed by fluorescence microscopy (Leica DMI3000B, Wetzlar, Germany).

2.6. Cell morphology assay

Cells were seeded on 24-well plates at a density of $3x10^3$ cells/cm^2, and cell morphology was assessed after 1, 3, 5 and 7 days of culture under expansion conditions (with DMEM media). Cells were washed twice with PBS, fixed with 4% PFA for 15 min and then permeabilized with a 0.1% Triton X-100 solution (Sigma-Aldrich) for 10 min. After permeabilization, cells were incubated with Phalloidin-TRITC (Sigma-Aldrich; dilution 1:250, 2 µg/ml) for 45 min in the dark. Then, cells were washed twice with PBS and counterstained with DAPI 1.5 µg/ml) for 5 min and then washed with PBS. Cells were imaged by fluorescence microscope (Leica DMI3000B).

2.7. Kinetics Assay

ATMSCs, BMMSCs, and PDLSCs were plated onto 12-well plates at different cell densities: 1.5 $x10^2$ cells/cm^2 (PDLSCs), 1.5 $x10^3$ cells/cm^2 and 3 $x10^3$ cells/cm^2 using DMEM + 10% FBS as growth medium. Cells were kept at 37ºC and 5% CO_2 in a humidified atmosphere and culture medium was changed every 3-4 days. At days 1, 3, 5, 7, 9 and 12, cells were harvested using a solution of 0.05% trypsin (Gibco). Cells were incubated with trypsin for 7 min at 37 °C and 5% CO_2. The reaction was stopped by adding DMEM+10% FBS. Cells were centrifuged at 1250 rpm for 7 min and resuspended in DMEM+10% FBS. Cells were counted using the Trypan Blue exclusion method (Gibco) to determine cell growth curves.

2.8. Quantitative Assessment of Osteogenic Potential

Metabolic Activity: After 21 days of osteogenic differentiation, medium was removed, cells were washed with PBS and the metabolic activity of MSCs was evaluated using AlamarBlue® cell viability reagent (Thermo Fischer Scientific) following the manufacturer's guidelines. Briefly, a 10% AlamarBlue® solution in culture medium was added to cells and incubated at 37°C for 3 h. Fluorescence intensity was measured in a microplate reader at an excitation/emission wavelength of 560/590 nm. Two donors were used for each cell type. Three samples were used for each condition and fluorescence was measured in triplicates.

ALP Activity Assay: After 21 days of osteogenic differentiation, ALP activity was detected using a colorimetric ALP kit (BioAssays Systems) according to the manufacturer's protocol. Samples were washed with PBS and incubated in lysis buffer composed by 0.1% Triton X-100 in PBS by shaking for 30 minutes at room temperature. The lysate was added to p-nitrophenyl phosphate solution (10 mM) provided with the ALP kit. Lastly, the absorbance was measured on a plate reader at 405 nm and normalized to the metabolic activity. Two donors were used for each cell type. Three different samples were used for each condition and absorbance was measured in triplicates.

Calcium Quantification Assay: For determination of total calcium content, samples were washed with PBS and incubated with a 0.5 M HCl solution (Sigma-Aldrich). Accumulated calcium was removed from the cellular component by shaking overnight at 4°C. The supernatant was used for calcium determination according to the manufacturer's instructions in the calcium colorimetric assay kit (Sigma-Aldrich). Total calcium was calculated from calcium standard solutions prepared in parallel. Absorbance at 575 nm was measured for each condition on a plate reader and normalized to the metabolic activity. Two donors were used for each cell type. Three samples were used for each condition and absorbance values were measured in triplicates.

Quantitative Reverse Transcription-Polymerase Chain Reaction (qRT-PCR) Analysis: Total RNA was extracted using the RNeasy Mini Kit (QIAGEN, Germany). cDNA was synthesized from the purified RNA using High-Capacity cDNA Reverse Transcription kit (Life Technologies). Reaction mixtures were incubated in a thermal cycler (Veriti 96-well thermal cycler: Applied Biosystems) for 5 min at 25 °C, 30min at 42 °C and 5min at 85 °C and then were maintained at 4 °C. The qRT-PCR was performed using NZYSpeedy qPCR Green Master Mix (2x), ROX plus (NZYTech) and StepOnePlus real-time PCR system (Applied Biosystems). All reactions were carried out at 95 °C for 10 min, followed by 40 cycles of 95 °C for 15 sec and 60°C for 1min; all were performed in triplicate. Target genes expression was primarily normalized to the housekeeping gene glyceraldehyde 3-phosphate dehydrogenase (GAPDH) and then determined as a fold-change relative to the baseline expression of the target genes measured at day 0 (undifferentiated cells) as internal control to normalize differences in total RNA levels in each sample. A threshold cycle (Ct) was observed in the exponential phase.

2.9. Fabrication of 3D Printed PCL Scaffolds by Fused Deposition Modeling

The scaffolds were fabricated using a 3D extrusion printing system (Prusa, i3 MK3) using fused deposition modelling technology. Three PCL (MW 50000 Da, ™ 6500, Perstorp Caprolactones) scaffolds with different sizes (100 µm, 300 µm and 600 µm) were designed by CAD in the form of squared prisms. Briefly, the PCL filament material was heated at 80º C (a temperature above PCL's melting point of 60º C) and extruded through a nozzle guided by a robotic device with computer-controlled motion. Each layer has a 0.15 mm height, and all layers were printed in a squared grid pattern.

2.10. Metabolic Activity and Morphology of PDLSCs cultured in 3D printed PCL Scaffolds

The metabolic activity of PDLSCs was evaluated on days 1, 3, 7 and 10 using AlamarBlue® cell viability reagent (Thermo Fischer Scientific) identically to previously described in section 2.8. Scaffolds without seeded cells (for each experimental group) were used as blank controls. Four scaffolds (n = 4) were analyzed for each experimental group and fluorescence values of each sample were measured in triplicate. Cell morphology was assessed using DAPI/Phalloidin staining, as described in section 2.6.

3. Results

3.1. PDLSC Isolation and Characterization

After successful isolation, PDLSCs attached to the culture plate and displayed a fibroblast-like morphology similar to MSCs. PDLSCs were then expanded *in vitro* and cells from passages 1-7 were used for the experiments presented below.

3.1.1. Expression of Mesenchymal Stromal Markers

Figure 1 depicts the immunophenotypic profile of PDLSCs assessed by flow cytometry. Results demonstrated positive expression of the MSC-associated markers CD29, CD44, CD73, CD90, and CD105. However, Stro-1 and CD106 were consistently negatively expressed by PDLSCs in passages 1-7. PDLSCs lack the expression of hematopoietic stem cell (HSC) markers and CD80, a co-stimulatory molecule essential for T-lymphocyte activation [13]. Lastly, PDLSCs also exhibited positive expression of CD146, an endothelial cell antigen also expressed at the surface of pericytes and previously used in the identification PDLSCs [9]. However, CD146 expression levels decreased with passaging.

3.1.2. Multilineage Differentiation

After 21 days of differentiation, successful *in vitro* differentiation of PDLSCs into adipo-, chondro- and osteogenic lineages (Figure 2) was confirmed. Adipogenic differentiation resulted in accumulation of lipid droplets, positively stained with Oil red O. Osteogenic differentiation was confirmed by ALP/VK staining, in which ALP synthesis is confirmed by the reddish areas and the deposition of minerals is observed by the black staining. Lastly, chondrogenic differentiation was confirmed by Alcian blue staining, confirming the presence of GAGs.

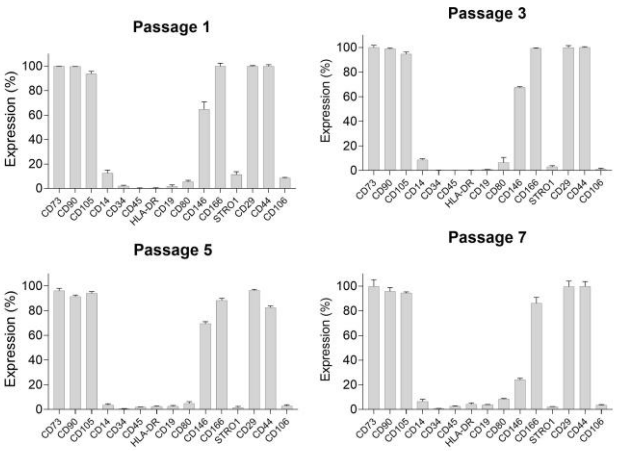

Figure 1. Surface marker expression by PDLSCs cultured in expansion conditions in passages 1, 3, 5 and 7. Data are expressed as mean ± SD (n=2, two donors).

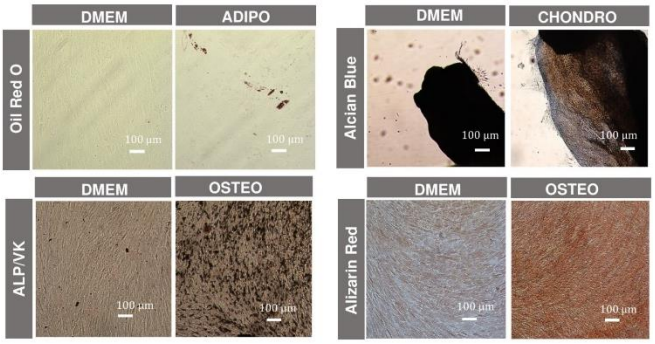

Figure 2. In vitro multilineage differentiation of PDLSCs. Adipogenic differentiation was detected by Oil red O staining. Chondrogenic differentiation was detected by Alcian blue. Alkaline phosphatase (ALP), von Kossa (VK) stainings and Alizarin Red confirmed osteogenic differentiation. As controls, all stainings were performed in PDLSCs cultured under expansion conditions (DMEM). Scale bar, 100 µm.

3.1.3. Growth Kinetics

To evaluate the proliferative capacity of PDLSCs, cells were plated at three different cell seeding densities: 1.5 x10^2 cells/cm^2, 1.5 x10^3 cells/cm^2 and 3 x10^3 cells/cm^2 (Figure 3) and counted at different timepoints (n=2, two donors). The growth kinetic curves for PDLSCs cultured at 1.5 x10^3 cells/cm^2 and 3 x10^3 cells/cm^2 displayed similar behavior. When seeded at 1.5 x10^2 cells/cm^2, PDLSCs remained in the adaptation phase for 5 days and the results indicated that, after 12 days of culture, PDLSCs were still in exponential growth phase, reaching (3.3 ± 1.3) x10^5 cells per well (Figure 3).

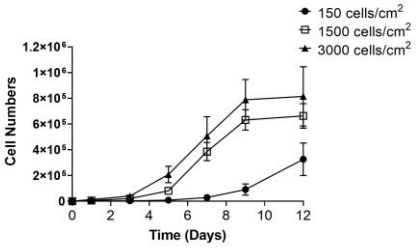

Figure 3. Growth curves of PDLSCs cultured at different cell seeding densities: 150, 1500 and 3000 cells/cm^2. Data are expressed as mean ± SD (n=2, two donors).

3.2. Comparison of MSCs derived from Adipose Tissue, Bone Marrow and Periodontal Ligament

3.2.1. Flow Cytometry

Immunophenotypic analysis of PDLSCs, BMMSCs and ATMSCs was assessed by flow cytometry (Figure 4). All samples displayed strongly positive expression (> 90%) of MSC-associated cell surface markers CD29, CD44, CD73, CD90, CD105, and CD166 in passage 3. Interestingly, CD44 expression levels of PDLSCs remained significantly high (> 99.7%), independently of passage number. Results showed that CD166 expression was positive (> 83.1%) for PDLSCs and BMMSCs in passages 3, 5 and 7. However, for ATMSCs, CD166 expression levels showed a tendency to decrease with passaging, presenting expression of (45.94 ± 2.65)% and (64.87 ± 5.12)% in passages 5 and 7, respectively.

CD106 and Stro-1 expression levels were low (< 10%) in all samples, irrespectively of cell source. As expected, all samples displayed negative expression of known HSC-related markers, namely CD14, CD19, CD34, CD45 and HLA-DR. Additionally, the immune cell-related marker CD80 was negatively expressed by samples from all MSC sources. Finally, results showed that CD146, a marker previously used to identify PDLSCs [9], was only expressed by PDLSCs. Despite this, results showed that CD146 expression by PDLSCs decreased with passaging ((64.8 ± 0.91)% for passage 1, (47.4 ± 1.6)% for passage 5 and (24.1 ± 1.2)% for passage 7). CD146 expression was absent in BMMSCs and ATMSCs.

3.2.2. Immunocytochemistry Analysis

Results depicted in Figure 5 confirmed the expression of the common ECM and cytoskeleton proteins, such as laminin and fibronectin, in all samples. Additionally, only PDLSCs expressed Stro-1, a known MSC marker [14], asporin, a protein associated with the PDL [15], osteocalcin and osteopontin, bone extracellular matrix proteins [16].

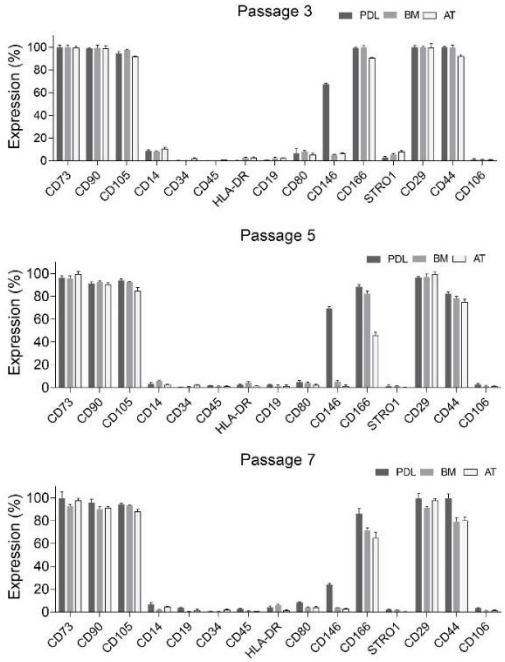

Figure 4. Immunophenotypic analysis of PDLSCs, ATMSCs and BMMSCs cultured in expansion conditions (DMEM + 10%FBS) at passages 3, 5 and 7 by flow cytometry. Data are expressed as mean ± SD (n=2, two donors per cell type).

3.2.3. Multilineage Differentiation

After 21 days of differentiation in adipo-, chondro-, and osteogenic media, appropriate staining confirmed the *in vitro* differentiation of PDLSCs, BMMSCs and ATMSCs into adipogenic, chondrogenic and osteogenic lineages (Figure 6). PDLSCs exhibited a lower number of Oil Red-O stained liquid droplets, suggesting a lower adipogenic potential compared with BMMSCs and ATMSCs.

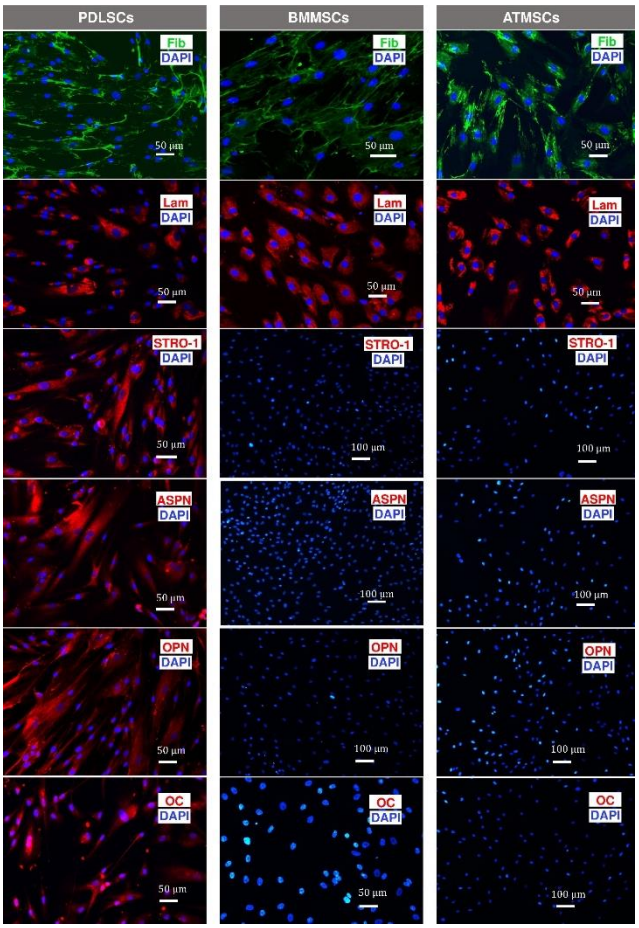

Figure 5. Comparison of immunofluorescent staining images for PDLSCs, BMMSCs and ATMSCs for the expression of fibronectin (Fib, green), laminin (Lam, red), stro-1 (STRO-1, red), asporin (ASPN, red), osteopontin (OPN, red) and osteocalcin (OC, red). Nuclei were stained with DAPI (blue).

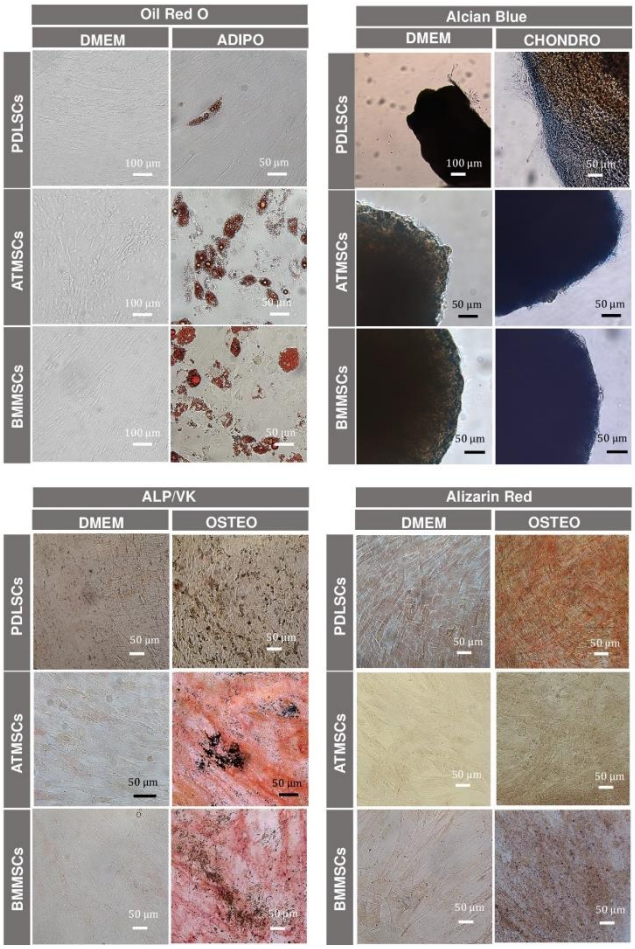

Figure 6. In vitro multilineage differentiation of PDLSCs, ATMSCs and BMMSCs. Adipogenic differentiation was detected with Oil red O staining showing the lipid vacuoles in red. Alcian blue stained aggregated chondrocytes in blue. Alkaline phosphatase (ALP) and von Kossa (VK) stainings showed ALP activity in red and mineralized extracellular matrix deposits in black. Alizarin red stained calcium deposits in the extracellular matrix in red. As controls, all stainings were also performed in expansion conditions (DMEM).

3.2.4. Growth Kinetics

Comparative growth kinetics studies were conducted with PDLSCs, BMMSCs and ATMSCs plated at 1.5 x10^3 and 3 x10^3 cells/cm^2 (Figure 7, n=2, two donors per cell type). Interestingly, PDLSCs reached around (7.9 ± 1.6) x10^5 cells at day 9 when seeded at 3 x10^3 cells/cm^2, while BMMSCs and ATMSCs only reached (5.4 ± 2.2) x10^4 and (8.3 ± 2.8) x10^4 cells, respectively. When cells were seeded at 1.5 x10^3 cells/cm^2, PDLSCs reached (6.3 ± 0.79) x10^5 cells, while BMMSCs and ATMSCs presented (2.9 ± 2.1) x10^4 and (9.4 x10^4 ± 0.13) x10^4 cells, respectively, at day 9. ATMSCs presented higher cell numbers than BMMSCs. Moreover, as observed in Figure 8, PDLSCs were able to reach higher population doublings after 9 days of cell culture compared to BMMSCs and ATMSCs (6.0 ± 0.3 *vs* 2.1 ± 0.6 and 2.8 ± 0.5 for PDLSCs *vs* BMMSCs and ATMSCs, respectively when cultured at 3 x10^3 cells/cm^2).

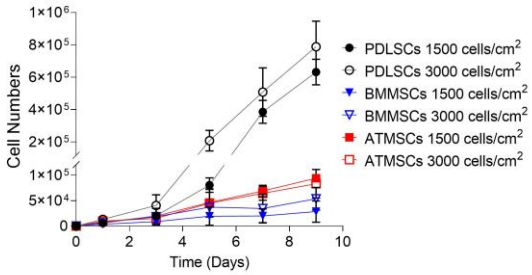

Figure 7. Growth curves of PDLSCs, ATMSCs and BMMSCs plated at 1500 and 3000 cells/cm^2. Data are expressed as mean ± SD (n=2, two donors per cell type).

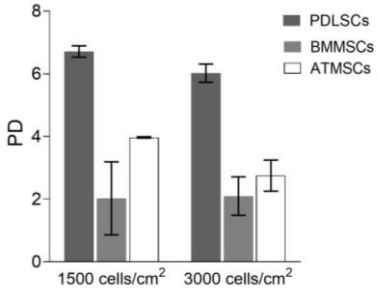

Figure 8. Population doublings (PD) of PDLSCs ATMSCs and BMMSCs plated at 1500 and 3000 cells/cm^2. Data are expressed as mean ± SD (n=2, two donors per cell type).

3.3. Osteogenic Potential of MSCs derived from Adipose Tissue, Bone Marrow and Periodontal Ligament

3.3.1. Calcium Quantification and ALP Activity

Figure 9 confirmed the successful osteogenic differentiation of MSCs from different sources, presenting higher calcium accumulation after osteogenic differentiation (OSTEO). Differentiated BMMSCs and ATMSCs presented similar values of calcium deposition after 21 days of osteogenic differentiation. However, a significant enhancement in calcium accumulation was observed by PDLSCs compared to BMMSCs and ATMSCs (1.72 x10^{-6} ± 2.0 µg.µL^{-1}). Regarding ALP activity, results demonstrated that ALP activity of PDLSCs did not increase after osteogenic differentiation ((1.4 ± 0.13) x10^{-4} µg.µL^{-1}). On the other hand, the ALP activity of BMMSCs and ATMSCs presented a significant increase after osteogenic differentiation (BMMSCs: (3.1 ± 0.26) x10^{-4} µg.µL^{-1}, ATMSCs: (2.7 ± 0.24) x10^{-4} µg.µL^{-1}).

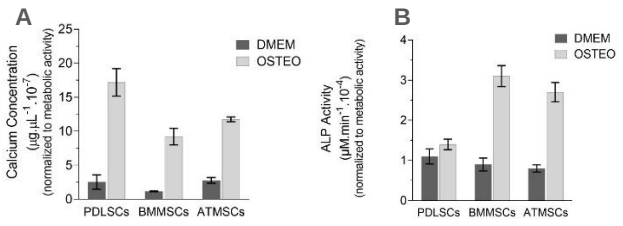

Figure 9. Calcium concentration and ALP Activity of PDLSCs, BMMSCs and ATMSCs cultured for 21 days under expansion (DMEM) and osteogenic differentiation (OSTEO) conditions. Data are expressed as mean ± SD (n=2, two different donors per cell type).

3.3.2. Gene Expression

Gene expression results demonstrated that PDLSCs have greater osteogenic potential compared to ATMSCs and BMMSCs, presenting enhanced upregulation of osteogenic/periodontal genes, such as *Col I*, *Runx2*, *OC*, *CEMP-1* and *POSTN* (Figure 10).

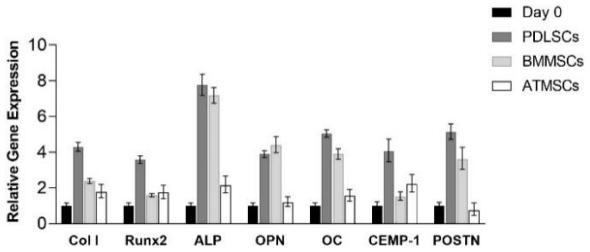

Figure 10. qRT-PCR analysis of PDLSCs, BMMSCs and ATMSCs after 21 days of osteogenic differentiation. Gene expression analysis of collagen I (Col I), RUNX family transcription factor 2 (Runx2), alkaline phosphatase (ALP), osteopontin (OPN), osteocalcin (OC), cementum protein-1 (CEMP-1) and periostin (POSTN). Data are expressed as mean ± SD (n=2, two donors per cell type).

3.3.3. Immunocytochemistry Analysis

Results depicted in Figure 11 revealed that MSCs derived from all sources stained positive for osteogenic -related markers, namely osteocalcin, osteopontin. Additionally, BMMSCs and PDLSCs expressed asporin, a periodontal-related marker. Interestingly, cementum protein-1 was exclusively expressed by PDLSCs.

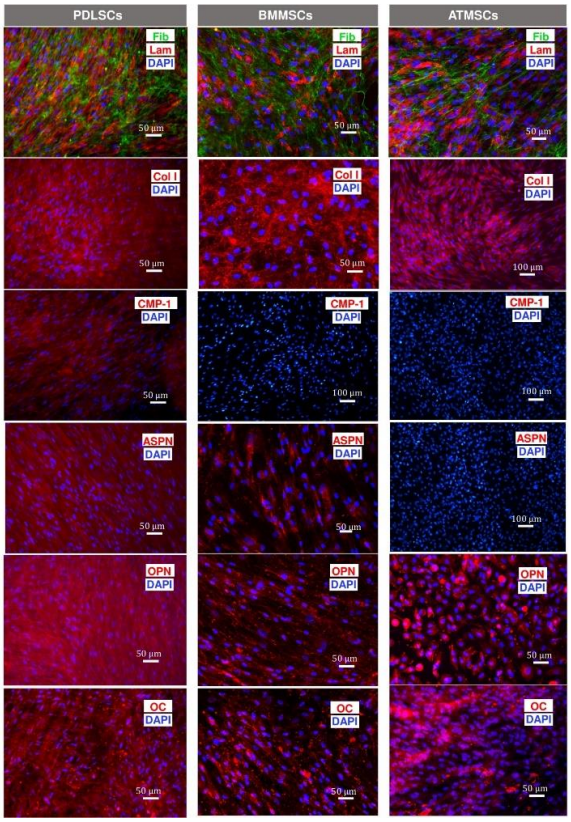

Figure 11. Immunocytochemistry analysis of PDLSCs, BMMSCs and ATMSCs cultured under osteogenic differentiation conditions for 21 days. Expression of fibronectin (Fib, green), laminin (Lam, red), collagen I (Col I, red), cementum protein-1 (CEMP-1, red), asporin (ASPN, red), osteopontin (OPN, red), and osteocalcin (OC, red).

3.4. PDLSC Culture on 3D Printed PCL Scaffolds

3.4.1. Cell Proliferation and Morphology

To evaluate the effect of scaffold pore size in PDLSCs proliferation, cells were seeded onto 3D printed PCL scaffolds with different pore sizes, namely 100 µm, 300 µm and 600 µm. PDLSCs were able to successfully adhere to the scaffold surface independently of scaffold pore size. PDLSCs were able to proliferate in all scaffolds during 10 days of culture. After 3 days of culture, cell numbers were comparable regardless of pore size. However, after 10 days of culture, cell numbers were considerably higher for 100 µm and 300 µm pore sizes than in the 600 µm pore scaffold (Figure 12).

Morphology of PDLSCs seeded onto 3D printed PCL scaffolds with different pore sizes was evaluated by DAPI/Phalloidin staining. PDLSCs demonstrated high proliferation on the scaffold surface, forming cell layers in all scaffolds.

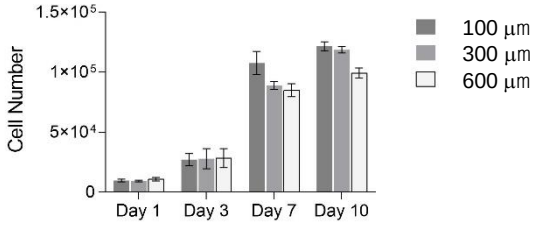

Figure 12. Proliferation of PDLSCs cultured for 10 days in expansion conditions (DMEM + 10% FBS) on polycaprolactone scaffolds with different pore sizes (100 µm, 300 µm and 600 µm).

4. Discussion

After successful PDLSC isolation, PDLSC characterization revealed positive expression of MSC-related surface markers CD29, CD44, CD73, CD90, CD105 (Figure 1)[17–20]. Despite previous studies reporting CD106 expression by MSCs[21], results showed that CD106 was absent in PDLSCs. In fact, previous studies also reported negative expression of CD106 by PDLSCs [22]. Interestingly, PDLSCs expressed CD166, a biomarker expressed by BMMSCs and lost during their development into differentiated phenotypes[20,23], (>99% in P1 through P5, and >50% for P6 and P7). As expected, and in agreement with previous studies [22,24–28], PDLSCs did not express HSC markers. PDLSCs have been reported to possess immunomodulatory properties similar to BMMSCs[22], thus, the negative expression of CD80, a T cell co-stimulatory molecule, suggested low immunogenicity [22,29,30]. CD146 is a cell surface marker previously used for identification of PDLSCs [9,31] and is commonly used as a marker of endothelial cells[32]. Interestingly, results showed that PDLSCs presented a high positive expression of CD146 while BMMSCs and ATMSCs did not. However, a significant decrease in CD146 expression was observed after passage 5. Therefore, these results demonstrated that high passage numbers of PDLSCs can influence the immunophenotype of PDLSCs. Nonetheless, more healthy donors are required to further investigate donor variability and its effect in immunophenotypic analysis.

Additionally, MSC phenotype was confirmed by successful PDLSC trilineage differentiation (adipogenic, chondrogenic and osteogenic

differentiation) (Figure 2). After 21 days of *in vitro* differentiation, PDLSCs exhibited an osteogenic phenotype, as confirmed by the presence of Alizarin Red-positive mineral deposits, which indicate calcium deposition. Chondrogenic potential of PDLSCs was confirmed by the positive Alcian blue staining of chondrocyte-specific matrix deposition. Lastly, results confirmed the adipogenic differentiation of PDLSCs by the presence of Oil Red O-positive cells with stained lipid vacuoles. These results are in line with BMMSC and PDLSC characterization [9,18,28,33-36] when exposed to similar culture conditions.

Growth kinetics results demonstrated that PDLSCs exhibited high proliferative capacity reaching (7.9 ± 1.6) $x10^5$ cells and (6.3 ± 0.79) $x10^5$ cells after 12 days of culture when cells were seeded at 1.5 $x10^3$ cells/cm^2 and 3 $x10^3$ cells/cm^2, respectively. Interestingly, results revealed that PDLSCs cultured at higher cell densities (1.5 and 3 $x10^3$ cells/cm^2) presented a lower growth rate in comparison to cells cultured at a lower cell density (1.5 $x10^2$ cells/cm^2) after 12 days (Figure 3). In fact, growth kinetic curve of PDLSCs cultured at lower cell density did not present a plateau after 12 days, suggesting that PDLSCs were still in an exponential growth phase.

Aiming to understand the differences between MSCs isolated from different sources, comparative studies with BMMSCs, ATMSCs and PDLSCs were performed. Overall, PDLSCs, BMMSCs and ATMSCs presented the typical MSC-associated properties, such as MSC-related surface marker expression and multilineage differentiation potential[18]. Nonetheless, phenotypical differences between the three cell types were identified, particularly in surface marker expression, protein synthesis and cell growth kinetics. As expected, and in line with previous reports, PDLSCs [22,24–26,35,37], BMMSCs [27,38–40] and ATMSCs [38,39,41,42] positively expressed MSC-related markers CD29, CD44, CD73, CD90, CD105 (Figure 4). ATMSCs showed a higher variation in CD166 expression levels when compared with PDLSCs and BMMSCs. We believe that these variations might be due to cell passage and donor variability. In fact, most of the results found in literature regarding immunophenotypic analysis of human BMMSCs and ATMSCs use cells in early passages. Therefore, further experiments with more donors are needed. Both BMMSCs and ATMSCs exhibited negative expression of CD146 in all passages (< 7 %). Interestingly, PDLSC expression of CD146 is positive, presenting CD146 expression levels of (67.4 ± 0.9) % in passage 3 and (69.5 ± 1.6) % in passage 5. However, CD146 expression of PDLSCs at passage 7 decreased (24.1 ± 1.2) %. These results suggested that CD146 expression could be used as a marker for PDLSCs, since BMMSCs and ATMSCs did not express CD146. Nevertheless, further experiments should include more donors to assess differences in CD146 expression between PDLSCs, BMMSCs and ATMSCs

Immunocytochemistry analysis of PDLSCs, BMMSCs and ATMSCs (Figure 5) confirmed the presence of commonly expressed ECM molecules laminin and fibronectin. Interestingly, Stro-1, a previously mentioned MSC-associated marker, was exclusively expressed by PDLSCs. As discussed above, literature suggests that Stro-1 expression by BMMSCs is markedly donor dependent, thus, negative immunofluorescence staining could be explained by donor variability. Contrary to the results presented in this work, previous immunocytochemistry studies have reported Stro-1 expression in ATMSCs [43,44], however, results showed preferential perivascular expression within adipose tissue [44] and an expression pattern highly specific for endothelial cells in arterioles and capillaries [43]. Interestingly, PDLSCs presented positive immunofluorescence stainings for asporin, osteopontin and osteocalcin (without osteogenic differentiation conditions), which were absent in BMMSCs and ATMSCs. These results may suggest a higher osteogenic potential presented by PDLSCs.

Comparison of PDLSCs, BMMSCs and ATMSCs growth curves revealed substantial differences in proliferation capacities of these cells (Figure 7). BMMSCs and ATMSCs exhibited similar growth patterns. Despite this, ATMSCs reached higher cell numbers than BMMSCs. Previous studies also reported that ATMSCs presented similar or greater rates of proliferation than BMMSCs [39,45,46]. PDLSCs exhibited a significant increase in proliferation capacity, reaching final cell numbers higher than BMMSC and ATMSC (PDLSCs: (7.9 ± 1.6) $x10^5$ cells, BMMSCs: (5.4 ± 2.2) $x10^4$ cells, ATMSCs: (8.3 ± 2.8) $x10^4$ cells). Moreover, PDLSCs exhibited higher population doublings after 9 days of culture, regardless of cell seeding density (Figure 8).

Osteogenic differentiation results confirmed that PDLSCs, BMMSCs and ATMSCs were able to differentiate into an osteogenic lineage. However, significant changes were observed in the osteogenic commitment during differentiation of PDL-, bone marrow- and adipose tissue-derived stem cells. Results presented in Figure 9 demonstrated that although calcium amount was similar for differentiated BMMSCs and ATMSCs, significant higher amount of calcium was presented in differentiated PDLSCs, suggesting an enhancement of osteogenic potential by MSCs derived from PDL. Furthermore, results demonstrated that ALP activity of PDLSCs did not increase after osteogenic differentiation. On the other hand, the ALP activity of BMMSCs and ATMSCs presented a significant increase after osteogenic differentiation. In fact, these results are in accordance with ALP staining results, confirming the low ALP activity of PDLSCs. We believe that the lack of ALP activity observed in this work might be due to the presence of a population of ALP^- cells, as reported by Yu and colleagues [47]. It is important to highlight that the lower levels of ALP activity of PDLSCs did not compromise the osteogenic differentiation of these cells, as observed by the enhancement of mineralization and upregulation of osteogenic marker genes. Interestingly, the low levels of ALP activity of PDLSCs might be related to the decreased adipogenic potential presented by PDLSCs. In fact, ALP is involved in the control of intracellular lipid accumulation in preadipocyte maturation, thus, absence of ALP may prevent formation of lipids in cells [48,49].

The role of PDLSCs in osteogenic differentiation has been widely studied *in vitro* and *in vivo*. Reports showed that a population of PDLSCs migrated from PDL remnants, upregulated osteogenic gene expression, differentiated into osteoblasts and generated new bone following tooth extraction [50]. Additionally, qRT-PCR results (Figure

10) demonstrated that after osteogenic differentiation, ATMSCs presented lower relative expression of osteogenic marker genes, compared to BMMSCs and PDLSCs. Overall, these results suggested that ATMSCs might possess lower osteogenic capacity compared with PDLSCs and BMMSCs. This is supported by previous comparative studies that reported limited osteogenic differentiation potential of ATMSCs compared to BMMSCs [38,39,46,51]. Additionally, PDLSCs presented higher upregulation of *Runx2* gene compared to BMMSCs and ATMSCs after 21 days of osteogenic differentiation. *RUNX2* is known to be crucial for the commitment of MSCs to an osteogenic lineage [52], regulating downstream genes that determine the osteogenic phenotype and controlling the expression of osteogenic marker genes, such as *Col I, ALP*, *OPN*, and *OC* [53,54]. Additionally, gene expression levels revealed higher upregulation of *Col I* and *CEMP-1* by PDLSCs compared with BMMSCs and ATMSCs. *Col I* is the most abundant protein in bone ECM and is pivotal for matrix mineralization [55] and *CEMP-1* has been identified as a novel cementum-specific protein [56]. Enhanced upregulation of *CEMP-1* gene expression suggested that PDLSCs may comprise a subpopulation of cementum progenitor cells, as previously proposed by McCulloch & Melcher in 1983 and further supported by recent studies [37,58].

Periostin has a key role as a modulator of PDL homeostasis [59] and in osteoblast adhesion, differentiation and survival [59,60]. After 21 days of osteogenic differentiation, PDLSCs presented higher periostin (*POSTN*) gene expression levels compared with BMMSCs. Considered periostin functions in the PDL, it is not surprising that osteogenic differentiated PDLSCs expressed higher levels of periostin as PDLSCs reside in the PDL.

After 21 days of osteogenic differentiation, immunocytochemistry stainings (Figure 11) showed positive expression of common ECM proteins, laminin and fibronectin. Additionally, positive stainings for osteopontin and osteocalcin were observed in ATMSCs, BMMSCs and PDLSCs. Asporin was observed in PDLSCs and BMMSCs, but not in ATMSCs. The strongly positive extracellular collagen I staining observable in all samples is consistent with an effective differentiation into an osteogenic lineage. Only differentiated PDLSCs revealed a positive staining for CEMP-1 expression. Other studies have reported CEMP-1 expression in osteogenic differentiated PDLSCs [61], however, it is still not clear if cementoblasts and osteoblasts arise from a common progenitor because both of these cell types share features of mineral-forming capacity and gene expression.

Design of scaffolds for periodontal Tissue Engineering applications requires understanding the relationship between structure and biological function. Here, we evaluated the impact of scaffolds' pore size in PDLSC proliferation. Results herein presented showed that PDLSCs are able to proliferate for 10 days in 3D printed PCL scaffolds (Figure 1), regardless of pore size (100, 300 and 600 µm). Results suggested that lower pore sizes (100 µm and 300 µm) favored higher proliferation rates. Furthermore, osteogenic differentiation assays, such as calcium quantification and qRT-PCR analysis, should be performed to further understand the impact of pore size in periodontal/osteogenic differentiation of PDLSCs.

5. Conclusions

The work herein presented provided additional evidences that PDL harbors a population of highly proliferative, multipotent stem cells that express the MSC phenotype (PDLSCs) as defined by the minimal criteria proposed by International Society for Cellular Therapy [18]. Moreover, this MSc Thesis contributed to the establishment of a standard, effective and reproducible protocol for the isolation and identification of PDLSCs in Stem Cell Engineering and Research Group laboratory in the (SCERG, iBB-IST, Portugal). Comparison of PDLSCs, ATMSCs and BMMSCs revealed phenotypic similarities regarding expression of MSC-related markers, contributing to the establishment of PDLSCs as a novel source of MSCs. Despite this, PDLSCs presented positive immunofluorescence stainings for asporin, osteopontin and osteocalcin, which were negatively stained in BMMSCs and ATMSCs. These results suggested that PDLSCs may have a higher osteogenic potential than BMMSCs and ATMSCs. Moreover, quantitative assessment of osteogenic differentiation potential confirmed that PDLSCs have higher osteogenic potential than BMMSCs and ATMSCs, presented increased calcium deposition and enhanced upregulation of osteogenic marker genes. Furthermore, positive immunofluorescence staining results showed that PDLSCs expressed CEMP-1 after osteogenic differentiation, suggesting that PDLSCs may comprise a subpopulation of cementum progenitor cells.

Overall, the results presented in this study suggested that PDLSCs are excellent candidates for periodontal tissue regeneration. PDLSCs possess high proliferative and osteogenic capacity, which constitutes an advantage for *ex-vivo* cell expansion and for alveolar bone regeneration. Regarding periodontal Tissue Engineering applications, results confirmed that 3D printed PCL scaffolds with different pore sizes (100 µm, 300 µm and 600 µm) are suitable for PDLSC proliferation, contributing to the development of novel patient-specific scaffolds for periodontal tissue regeneration.

6. Future Perspectives

The development of a scaffold-based therapy combined with the delivery of MSCs to promote alveolar bone tissue regeneration may contribute to significant advancements in periodontal tissue regeneration. To achieve such goals, further characterization of PDLSCs is necessary to identify reliable PDLSC-specific markers. Moreover, additional investigation of osteogenic differentiation mechanisms in PDLSCs should be carried out to further understand the PDLSC functions in alveolar bone regeneration.

Future studies regarding the development of a new scaffold-based therapy for periodontal tissue regeneration must include further optimization of PCL scaffold's pore sizes to determine the most

favorable pore size for PDLSC proliferation and osteogenic differentiation. Furthermore, scaffold seeding efficiency should be improved. New polymers for alveolar bone support while accelerating bone regeneration should be investigated. Finally, periodontal tissue regeneration can only be fully achieved with coordinated regeneration of PDL, cementum and alveolar bone [62]. Thus, multiphasic scaffold approaches, with each layer/phase designed to guide a specific target tissue regeneration, should be also explored. For instance, a complex scaffold with an alveolar bone phase with FDM 3D printed scaffolding, an intermediate phase with a fibrous filling to aid in PDL regeneration, and a third thin phase to promote new cementum formation.

References

1. Nanci, A. & Bosshardt, D. D. Structure of periodontal tissues in health and disease. *Periodontol. 2000* **40**, 11–28 (2006).
2. Grzesik, W. J. & Narayanan, A. S. Cementum and Periodontal Wound Healing and Regeneration. *Crit. Rev. Oral Biol. Med.* **13**, 474–484 (2002).
3. Liu, H. W., Yacobi, R., Savion, N., Narayanan, A. S. & Pitaru, S. A Collagenous Cementum-Derived Attachment Protein Is a Marker for Progenitors of the Mineralized Tissue-Forming Cell Lineage of the Periodontal Ligament. *J. Bone Miner. Res.* **12**, 1691–1699 (1997).
4. Kinane, D. F., Stathopoulou, P. G. & Papapanou, P. N. Periodontal diseases. *Nat. Rev. Dis. Prim.* **3**, 17038 (2017).
5. Pihlstrom, B. L., Michalowicz, B. S. & Johnson, N. W. Periodontal diseases. *Lancet (London, England)* **366**, 1809–20 (2005).
6. Preshaw, P. M., Seymour, R. A. & Heasman, P. A. Current Concepts in Periodontal Pathogenesis. *Dent. Update* **31**, 570–578 (2004).
7. Melcher, A. H. Cells of periodontium: their role in the healing of wounds. *Ann. R. Coll. Surg. Engl.* **67**, 130–1 (1985).
8. Bartold, P. M., Shi, S. & Gronthos, S. Stem cells and periodontal regeneration. *Periodontol. 2000* **40**, 164–172 (2006).
9. Seo, B. *et al.* Investigation of multipotent postnatal stem cells from human periodontal ligament. 149–155 (2004) doi:10.1016/S0140-6736(04)16627-0.
10. Mrozik, K., Gronthos, S., Shi, S. & Bartold, P. M. A Method to Isolate, Purify, and Characterize Human Periodontal Ligament Stem Cells. in 413–427 (2017). doi:10.1007/978-1-4939-6685-1_24.
11. dos Santos, F. *et al.* Ex vivo expansion of human mesenchymal stem cells: A more effective cell proliferation kinetics and metabolism under hypoxia. *J. Cell. Physiol.* n/a-n/a (2009) doi:10.1002/jcp.21987.
12. Gimble, J. M., Katz, A. J. & Bunnell, B. A. Adipose-Derived Stem Cells for Regenerative Medicine. *Circ. Res.* **100**, 1249–1260 (2007).
13. Suvas, S., Singh, V., Sahdev, S., Vohra, H. & Agrewala, J. N. Distinct Role of CD80 and CD86 in the Regulation of the Activation of B Cell and B Cell Lymphoma. *J. Biol. Chem.* **277**, 7766–7775 (2002).
14. Simmons, P. J. & Torok-Storb, B. Identification of stromal cell precursors in human bone marrow by a novel monoclonal antibody, STRO-1. *Blood* **78**, 55–62 (1991).
15. Yamada, S., Kitamura, M. & Murakami, S. PLAP-1: A novel molecule regulating homeostasis of periodontal tissues. *Jpn. Dent. Sci. Rev.* **44**, 137–144 (2008).
16. Stein, G. S., Lian, J. B. & Owen, T. A. Relationship of cell growth to the regulation of tissue-specific gene expression during osteoblast differentiation. *FASEB J.* **4**, 3111–23 (1990).
17. Costa, P. F. *et al.* Advanced tissue engineering scaffold design for regeneration of the complex hierarchical periodontal structure. *J. Clin. Periodontol.* **41**, 283–294 (2014).
18. Dominici, M. *et al.* Minimal criteria for defining multipotent mesenchymal stromal cells. The International Society for Cellular Therapy position statement. *Cytotherapy* **8**, 315–317 (2006).
19. Goodwin, H. S. *et al.* Multilineage differentiation activity by cells isolated from umbilical cord blood: expression of bone, fat, and neural markers. *Biol. Blood Marrow Transplant.* **7**, 581–8 (2001).
20. Stewart, K. *et al.* STRO-1, HOP-26 (CD63), CD49a and SB-10 (CD166) as markers of primitive human marrow stromal cells and their more differentiated progeny: a comparative investigation in vitro. *Cell Tissue Res.* **313**, 281–290 (2003).
21. Yang, Z. X. *et al.* CD106 Identifies a Subpopulation of Mesenchymal Stem Cells with Unique Immunomodulatory Properties. *PLoS One* **8**, e59354 (2013).
22. Wada, N., Menicanin, D., Shi, S., Bartold, P. M. & Gronthos, S. Immunomodulatory properties of human periodontal ligament stem cells. *J. Cell. Physiol.* **219**, 667–676 (2009).
23. Bruder, S. P., Horowitz, M. C., Mosca, J. D. & Haynesworth, S. E. Monoclonal antibodies reactive with human osteogenic cell surface antigens. *Bone* **21**, 225–235 (1997).
24. Iwata, T. *et al.* Validation of human periodontal ligament-derived cells as a reliable source for cytotherapeutic use. *J. Clin. Periodontol.* **37**, 1088–1099 (2010).
25. Lindroos, B. *et al.* Characterisation of human dental stem cells and buccal mucosa fibroblasts. *Biochem. Biophys. Res. Commun.* **368**, 329–335 (2008).
26. Nagatomo, K. *et al.* Stem cell properties of human periodontal ligament cells. *J. Periodontal Res.* **41**, 303–310 (2006).
27. Tamaki, Y., Nakahara, T., Ishikawa, H. & Sato, S. In vitro analysis of mesenchymal stem cells derived from human teeth and bone marrow. *Odontology* **101**, 121–132 (2013).
28. Vasandan, A. B. *et al.* Functional differences in mesenchymal stromal cells from human dental pulp and periodontal ligament. *J. Cell. Mol. Med.* **18**, 344–354 (2014).
29. Ding, G. *et al.* Allogeneic Periodontal Ligament Stem Cell Therapy for Periodontitis in Swine. *Stem Cells* **28**, 1829–1838 (2010).
30. Li, X. *et al.* The effect of aging on the biological and immunological characteristics of periodontal ligament stem cells. *Stem Cell Res. Ther.* **11**, 326 (2020).
31. Saito, Y. *et al.* CD146/MCAM Surface Marker for Identifying Human Periodontal Ligament-derived Mesenchymal Stem Cells. *J. Hard Tissue Biol.* **22**, 115–128 (2013).
32. Guezguez, B. *et al.* Dual Role of Melanoma Cell Adhesion Molecule (MCAM)/CD146 in Lymphocyte Endothelium Interaction: MCAM/CD146 Promotes Rolling via Microvilli Induction in Lymphocyte and Is an Endothelial Adhesion Receptor. *J. Immunol.* **179**, 6673–6685 (2007).
33. Yang, Y.-H. K., Ogando, C. R., Wang See, C., Chang, T.-Y. & Barabino, G. A. Changes in phenotype and differentiation potential of human mesenchymal stem cells aging in vitro. *Stem Cell Res. Ther.* **9**, 131 (2018).
34. Gay, I., Chen, S. & MacDougall, M. Isolation and characterization of multipotent human periodontal ligament stem cells. *Orthod. Craniofac. Res.* **10**, 149–160 (2007).
35. Banavar, S. R. *et al.* Establishing a technique for isolation and characterization of human periodontal ligament derived mesenchymal stem cells. *Saudi Dent. J.* (2020) doi:10.1016/j.sdentj.2020.04.007.
36. Menicanin, D. *et al.* Periodontal-Ligament-Derived Stem Cells Exhibit the Capacity for Long-Term Survival, Self-Renewal, and Regeneration of Multiple Tissue Types in Vivo. *Stem Cells Dev.* **23**, 1001–1011 (2014).
37. Shinagawa-Ohama, R., Mochizuki, M., Tamaki, Y., Suda, N. & Nakahara, T. Heterogeneous Human Periodontal Ligament-Committed Progenitor and Stem Cell Populations Exhibit a Unique Cementogenic Property Under In Vitro and In Vivo Conditions. *Stem Cells Dev.* **26**, 632–645 (2017).
38. Xu, L. *et al.* Tissue source determines the differentiation potentials of mesenchymal stem cells: a comparative study of human mesenchymal stem cells from bone marrow and adipose tissue. *Stem Cell Res. Ther.* **8**, 275 (2017).
39. Mohamed-Ahmed, S. *et al.* Adipose-derived and bone marrow mesenchymal stem cells: a donor-matched comparison. *Stem Cell Res. Ther.* **9**, 168 (2018).
40. Wang, X. *et al.* Expression of CD44 standard form and variant isoforms in human bone marrow stromal cells. *Saudi Pharm. J.* **25**, 488–491 (2017).
41. Strem, B. M. *et al.* Multipotential differentiation of adipose tissue-derived stem cells. *Keio J. Med.* **54**, 132–141 (2005).
42. Petrenko, Y. *et al.* A Comparative Analysis of Multipotent Mesenchymal Stromal Cells derived from Different Sources, with a Focus on Neuroregenerative Potential. *Sci. Rep.* **10**, 4290 (2020).
43. Lin, G. *et al.* Tissue Distribution of Mesenchymal Stem Cell Marker Stro-1. *Stem Cells Dev.* **20**, 1747–1752 (2011).
44. Zannettino, A. C. W. *et al.* Multipotential human adipose-derived stromal stem cells exhibit a perivascular phenotype in vitro and in vivo. *J. Cell. Physiol.* **214**, 413–421 (2008).
45. LI, X. *et al.* Comprehensive characterization of four different populations of human mesenchymal stem cells as regards their immune properties, proliferation and differentiation. *Int. J. Mol. Med.* **34**, 695–704 (2014).
46. Shafiee, A. *et al.* A comparison between osteogenic differentiation of human unrestricted somatic stem cells and mesenchymal stem cells from bone marrow and adipose tissue. *Biotechnol. Lett.* **33**, 1257–1264 (2011).
47. Yu, Z. & Philippe, G. Differential Properties of Human ALP+ Periodontal Ligament Stem Cells vs Their ALP- Counterparts. *J. Stem Cell Res. Ther.* **05**, (2015).
48. Ali, A. T. *et al.* The relationship between alkaline phosphatase activity and intracellular lipid accumulation in murine 3T3-L1 cells and human preadipocytes. *Anal. Biochem.* **354**, 247–254 (2006).
49. Ali, A. *et al.* Lipid accumulation and alkaline phosphatase activity in human preadipocytes isolated from different body fat depots. *J. Endocrinol. Metab. Diabetes South Africa* **18**, 58–64 (2013).
50. Yuan, X. *et al.* A Wnt-Responsive PDL Population Effectuates Extraction Socket Healing. *J. Dent. Res.* **97**, 803–809 (2018).
51. Woo, D.-H., Hwang, H. S. & Shim, J. H. Comparison of adult stem cells derived from multiple stem cell niches. *Biotechnol. Lett.* **38**, 751–759 (2016).
52. Bruderer, M., Richards, R. G., Alini, M. & Stoddart, M. J. Role and regulation of RUNX2 in osteogenesis. *Eur. Cell. Mater.* **28**, 269–86 (2014).
53. Hayrapetyan, A., Jansen, J. A. & van den Beucken, J. J. J. P. Signaling pathways involved in osteogenesis and their application for bone regenerative medicine. *Tissue Eng. Part B. Rev.* **21**, 75–87 (2015).
54. Birmingham, E. *et al.* Osteogenic differentiation of mesenchymal stem cells is regulated by osteocyte and osteoblast cells in a simplified bone niche. *Eur. Cells Mater.* **23**, 13–27 (2012).
55. Lian, J. B. & Stein, G. S. Development of the osteoblast phenotype: molecular mechanisms mediating osteoblast growth and differentiation. *Iowa Orthop. J.* **15**, 118–40 (1995).
56. Arzate, H., Olson, S. W., Page, R. C., Gown, A. M. & Narayanan, A. S. Production of a monoclonal antibody to an attachment protein derived from human cementum. *FASEB J.* **6**, 2990–2995 (1992).
57. McCulloch, C. A. G. & Melcher, A. H. Cell density and cell generation in the periodontal ligament of mice. *Am. J. Anat.* **167**, 43–58 (1983).
58. Torii, D., Konishi, K., Watanabe, N., Goto, S. & Tsutsui, T. Cementogenic potential of multipotential mesenchymal stem cells purified from the human periodontal ligament. *Odontology* **103**, 27–35 (2015).
59. Romanos, G. E., Asnani, K. P., Hingorani, D. & Deshmukh, V. L. PERIOSTIN: role in formation and maintenance of dental tissues. *J. Cell. Physiol.* **229**, 1–5 (2014).
60. Horiuchi, K. *et al.* Identification and characterization of a novel protein, periostin, with restricted expression to periosteum and periodontal ligament and increased expression by transforming growth factor beta. *J. Bone Miner. Res.* **14**, 1239–49 (1999).
61. Komaki, M. *et al.* Cementum protein 1 (CEMP1) induces a cementoblastic phenotype and reduces osteoblastic differentiation in periodontal ligament cells. *J. Cell. Physiol.* **227**, 649–657 (2012).
62. Woo, H. N., Cho, Y. J., Tarafder, S. & Lee, C. H. The recent advances in scaffolds for integrated periodontal regeneration. *Bioact. Mater.* **6**, 3328–3342 (2021).